Soil Moisture and Rainfall Interplay for Tropical Ecosystems in The West African Terrain Using Satellite-Based Datasets and Gauge measurements

Prince Junior Asilevi (ev_asilevi@yahoo.com)
Ghana Meteorological Agency
Felicia Dogbey
Kwame Nkrumah University of Science and Technology
Emmanuel Quansah
Kwame Nkrumah University of Science and Technology
Deborah Amuzu
AGRHYMET

Research Article

Keywords: Soil moisture, Rainfall, NASA - POWER, tropical ecosystems, Ghana -West Africa

Posted Date: March 10th, 2022

DOI: https://doi.org/10.21203/rs.3.rs-1415367/v1

Abstract

The interplay of soil moisture (SM) and rainfall (RR) has practical importance for pluvial flood prevention and prediction, drought monitoring, and weather forecasting for agricultural applications. Recent satellite products have shown complicated SM - RR relationships over varied ecosystems, with a diverse range of positive to negative correlation indices. This study presents an assessment of the SM - RR interplay over contrasting tropical ecosystems across Ghana in the West Africa terrain, using RR gauge measurements and satellite-based root zone SM for 22 Synoptic stations spanning 30 years (1990–2019). Spatiotemporal distributions, percentage changes about onset dates, and statistical strength of correlations are presented and discussed. Findings show that, generally, SM decreases northward by a gradient of 0.01, showing weak to strong correlations of 0.38–0.82 ± 0.10 with RR countrywide, the highest is found for stations in the northern Savannah and Coastal Savannah zones, the weakest for stations in the Forest zone. Meanwhile, based on the RR onset dates, the Coastal zone exhibits the highest percentage change in SM, whereas the Forest, Transition, and Savannah zones exhibit low to slightly negative percentage changes. This has been attributed to SM deficits resulting from the dry Harmattan season before RR onset, strongly suggesting a respective delineation of Coastal and Savannah regions as flood and drought-prone zones. The results are in tandem with global-scale assessments, and present a theoretical framework to develop ecosystem water and pluvial flood management schemes over the sub-region.

1. Introduction

Soil moisture (SM) has emerged as an important environmental and climatic factor contributing significantly to climate change as the key driver of land-atmosphere energy fluxes via its composite effect on soil reflectivity, emissivity, and thermal capacity [1, 2]. Due to the influence of SM on near-to-surface air temperature and its feedback effect on rainfall, it is used to forecast the weather, monitor drought development, predict pluvial floods, as well as manage arable lands for agricultural use [3, 1, 4]. Moreover, it is estimated that on a global scale, nearly 70–90% of rainfall (RR) returns to the atmosphere via evapotranspiration (ET), making SM, RR, and ET critical requirements for the analysis, monitoring, and management of ecosystem water resources. Therefore, understanding the SM - RR dynamics, is the route to efficient water management and ecosystem preservation [5, 6].

Nevertheless, the SM - RR interplay remains a subject rarely explored mainly due to difficulties in consistent ET and SM measurements and the immersed spatiotemporal variability making point measurements of little relevance, especially for regional studies. Due to this, many studies on SM and ET rely on satellite observation [5, 7, 8]. In addition, RR has globally become an increasingly erratic event such that soil water content has attained a critical status for agriculture, especially during the lean-to-onset seasons [9]. However, this situation is expected to worsen as changes in land cover have been occurring rapidly on a global scale, mainly as a result of urbanization, industrialization, and increasing population in limited areas [10].

Antecedent satellite-based global studies on the SM - RR interplay have provided useful information and a template for regional and zonal considerations. For example, [11] reported global complexities in the SM - RR interplay using datasets retrieved from the National Aeronautics and Space Administration (NASA), specifically SM and RR from the Soil Moisture Active Passive (SMAP) and Tropical Rainfall Measuring Mission (TRMM) satellites respectively. The study observed that whereas SM correlates moderately well with RR for most regions globally, the correlation index is stronger for arid, warm, and low vegetation regions, and weaker for highly forested vegetation, humid, and temperate regions. Pan [1] reported similar complexities, and additionally significant changing trends on a seasonal scale, with satellite reanalysis datasets retrieved from the European Space Agency (ESA) and the Multi-Source Weighted-Ensemble Precipitation (MSWEP) climatological archives at $0.25^o \times 0.25^o$ spatial resolution and spanning 1979–2016. Meanwhile, some recent studies have reported negative SM - RR correlations for some dry soil regions in South Africa [12, 1], where strong convective activities cause much rainfall and consequential increased risk of pluvial floods [13]. This phenomenon has sternly raised questions to the traditional assertion that, “wet regions get wetter, dry regions get drier”, creating uncertainties on the SM - RR relationship.

The current study focuses on the Sub-Saharan West African region, interlocked between the Gulf of Guinea and the vast Sahara Desert, reportedly widening southward by nearly 100 km per satellite-assisted new evidence, which possess significant ecosystem threat to the region, with an expected increase in droughts and floods, along with temperature rise northward [14–16]. The aim is to assess the SM - RR interplay for contrasting tropical ecosystems across Ghana in Sub-Saharan West Africa, using daily SM datasets retrieved from the National Aeronautics and Space Administration - Prediction of Worldwide Energy Resources (NASA/ POWER) agro-climatological archives, and daily gauge RR measurement datasets spanning 1990–2019. This study also seeks to ascertain the characteristics of the interplay peculiar to the region, and the implication on possible floods and droughts. This work presents the first-ever attempt to couple NASA’s MERRA-2 SM retrievals with gauge measurements for the sub-region, and by the assumption that NASA’s MERRA-2 datasets will show SM where RR is recorded by surface gauge, RR will be used to informally validate the accuracy of SM datasets.

2. Materials And Methods

2.1. Geography and climatology of the study area

The study area, Ghana, is situated in the South Western African coastal territory shown in Fig. 1 and located precisely in latitude 4.5^o N and 11.5^o N and longitude 3.5^o W and 1.5^o E. Sharing geographical boundaries with Cote d’Ivoire, Togo, Burkina Faso, and the Gulf of Guinea to the West, East, North, and South respectively. The total land coverage is ~ 240,000 km^2, the prevailing climate is the typical West African Monsoon (WAM) driven by the oscillatory transition of the Intertropical Convergence Zone (ITCZ) over the region [17, 18].

Table 1: Names, codes, geographical positions, and elevations for selected synoptic stations. Station codes are as designated by the World Meteorological Organization (WMO) with Prefix-654

Station	Station code	Latitude (°)	Longitude (°)	Elevation (m)
Savannah				
Wa	04	10.05	-2.50	305.00
Navrongo	01	10.90	-1.10	197.00
Bole	16	9.33	-2.48	246.90
Tamale	18	9.42	-0.85	152.00
Yendi	20	9.45	-0.17	157.00
Transition				
Wenchi	32	7.75	-2.10	299.00
Sunyani	39	7.33	-2.33	305.00
Kete Krachi	37	7.82	-0.33	92.00
Forest				
Kumasi	42	6.72	-1.60	256.00
Sefwi Bekwai	45	6.20	-2.33	186.50
Oda	57	5.93	-0.98	151.00
Abetifi	50	6.67	-0.75	601.00
Koforidua	59	6.83	-0.25	199.00
Ho	53	6.60	0.47	154.00
Akuse	60	6.10	0.12	107.60
Axim	65	4.90	-2.25	71.00
Takoradi	67	4.88	-1.77	74.00
Coastal				
Salt Pond	69	5.20	-1.67	77.00
Accra	72	5.60	-0.17	91.00
Tema	73	5.62	0.00	79.00
Ada	75	5.78	0.63	15.30
Akatsi	62	6.12	0.80	66.50

For this study, the climatology and topography across the contrasting ecosystems of the study area relating to rainfall and soil moisture distributions respectively are considered. Climatologically, the WAM season stretches from March through to October, during which the southernmost half experiences a two-regime rainfall season separated by a brief dry season. The earlier rainfall season is the major regime running from March to June and is characterized by isolated heavy downpours predominantly over the west coast (see Fig. 1) in May. The ITCZ and consequential increased rainfall shift northward in June-July, resulting in increased cloud formation countrywide. The coastal south now experiences a brief dryness during June-July-August with the ITCZ shifted northwards, where outflows from deep convective activities occur accounting for a relatively longer single-regime rainfall over the northern half. Finally, the ITCZ oscillates backward into the southern coast by September-October-November, commencing a second but lean rainfall season [19–21]. Overall, two main seasons - wet and dry - characterize the area of study. Due to the highly variable nature of rainfall distribution and consequential climatic conditions in different parts of the region, the Ghana Meteorological Agency (GMet) recognizes four main climatic zones, namely the Savannah, Transition, Forest, and Coastal zones as shown in Fig. 1, as well as four main rainfall-related seasons viz December-January-February (DJF), March-April-May (MAM), June-July-August (JJA), and September-October-November (SON) [17, 18].

Furthermore, important to the consideration of SM - RR interplay, is the topography of the study area [22, 23]. The elevations for the study sites shown in Table 1, is evident that the study area shows a distinctly wide range of complex topographic terrains, characterized by highlands predominantly over the northern half Savannah and Transition zones, and forested mountain-ranges over the in-land Forest zone, while the Coastal zone exclusively maintains a lowland region.

Generally, except for the Kwahu Plateau in the southernmost forested zone (~ 14 km from Abetifi to the west, see Fig. 1), stretching along the Volta River Basin - the topography is relatively flat and low-lying, with over half the study area less than 150 m above mean sea level [24].

2.2. Data

2.2.1. Ground-based gauge measurement datasets

A collage of 30 years of daily surface rainfall (RR) measurements archived between 1990–2019 for the twenty-two (22) Synoptic stations in Fig. 1, distributed within the four main agro-climatic zones of the study area, were obtained from the Ghana Meteorological Agency (GMet) for the study. The daily rainfall datasets were measured by twenty-two (22) gauges. These stations have not suffered location changes, and gauge measurements were all quality control checked for the whole period before being received, by ensuring strict adherence to the rainfall climatology: bi-modal and mono-modal rainfall regimes in the southern half (Coastal and Forest zones) and northern half (Transition and Savannah zones) respectively [19]. Further, rainfall data were checked for reasonable ranges during the wet (June-July-August) and dry (November-December-January) seasons. For climate impact studies, the twenty-two (22) gauge datasets were grouped into the same four main agro-ecological zones that have been used in previous studies [17],

which are homogeneous in terms of rainfall regimes. Gauges forming these zones - referred to hereafter as Savannah, Transition, Forest, and Coastal are marked in Fig. 1.

2.2.2. Satellite-based soil moisture datasets

The long-term root zone soil moisture (SM) at 100 cm depth (SM_{100}) datasets corresponding to the 22 synoptic stations, used for this study was retrieved from the National Aeronautics and Space Administration - Prediction of Worldwide Energy Resources (NASA/ POWER) agro-climatological archives via user-friendly web-based mapping portal (https://power.larc.nasa.gov/data-access-viewer/).

The archive is fed-in by the Modern Era Retrospective-Analysis for Research and Applications, version 2 (MERRA-2) assimilation model products, which provided global SM reanalysis as point datasets spanning equal study period (1990–2019), accessible on a daily and monthly temporal resolution scale at $0.5^o \times 0.5^o$ spatial resolution [25, 26].

The MERRA-2 SM datasets have been quality controlled, validated, and shown to have good agreement indices compared with a global network of surface observation from the U.S. Department of Agriculture (USDA) Soil Climate Analysis Network (SCAN), the U.S. Climate Reference Network (USCRN), the Soil Moisture Ocean Salinity Meteorological Automatic Network Integrated Application (SMOSMANIA) sites in southwestern France (Albergel), and the OzNet network in Australia's Murrumbidgee catchment [25].

The NASA/ POWER MERRA-2 based SM_{100} is presented as dimensionless fractions with a value of 1 indicating complete soil saturation, and a value of 0 indicating complete water-free soil.

2.3. Statistical methods for analysis

In order to assess the strength of correlation between SM and RR, the standard deviation (σ) and Pearson's correlation (r) were applied on n number of observations as in Equations 1 and 2 based on [27, 28]:

$$\sigma = \sqrt{\frac{1}{n-1}\sum_{i=1}^{n}([SM, RR] - \mu)^2} \quad (1)$$

$$r = \frac{\sum_{i=1}^{n}(SM - \sigma_{SM})\,(RR - \sigma_{RR})}{(n-1)\,\sigma_{SM}\sigma_{RR}} \quad (2)$$

The standard deviation (σ) was used to check the upper and lower limits of distribution around the mean SM and RR, while Pearson's correlation coefficient (r) was used to quantify the strength of correlation between SM and RR.

3. Results And Discussions

3.1. Spatiotemporal distribution of soil moisture and rainfall

In order to assess the dynamism in relationship and response characteristics of soil moisture (SM) and rainfall (RR), the spatiotemporal distribution of SM and RR over the study area is discussed. Figures 2a and 2b display a climatological 30 years daily averages of ground-based RR gauge measurements and the NASA - POWER satellite-derived SM respectively, spanning 1990–2019 at the 22 synoptic stations in Fig. 1, distributed across the four main climatic zones. The advantage of Fig. 2 is that it displays simultaneously the space and time distributions. It is observed that generally on a spatial scale SM is highest over the southern half where RR is bimodal and lowest over the northern half where RR is mono-modal. On a temporal scale over the southern half, SM peaks from late May - July (~ 150–200th Julian days) immediately following the MAM major RR season (~ 60–150th Julian days), after which another very faint peak (~ 275–330th Julian days) follows the minor SON RR season (~ 250–300th Julian days), and eventually diminishes during the DJF dry season (~ 334–90th Julian days) when RR is lowest countrywide. Over the northern half, SM is generally low, showing a faint peak (~ 250–300th Julian days) following the long-range mono-modal RR season (~ 133–300th Julian days). These concurrent patterns establish the axiom that elevated RR is associated with elevated SM levels. However, there is high variability and significant contrasting SM - RR relationships across the varied ecoregions, creating room for other elements contributing to SM levels such as topography as noted in other studies [22, 23].

Firstly, over the southern half, a high daily mean SM > 0.70 ± 0.07 is mainly associated with coastal stations categorized into Forest climate towards the west-coast and Coastal Savannah-type climate towards the east-coast (see Fig. 1). Despite the high annual cumulative RR ~ 1500 mm over the west-coast relative to the lower RR ~ 700 mm over the east-coast [29], SM levels along the entire coastal stretch are higher. This can be attributed to two obvious reasons viz., elevated RR (relating to the west-coast) and the low-land topographic characteristics < 100 m (see Table 1) causing high seawater intrusion and percolation, and consequential strong weathering, high leaching, and low pH [24, 30]. However, over the northern half, stations show relatively lower daily mean SM between 0.46–0.56 ± 0.06, with a mono-modal RR pattern of an annual total amount ranging between 962.4–1198.9 ± 85.8 mm. The low zonal and seasonal RR/ SM is expected to cause quick responses in SM - RR relationship.

The northern half - mainly the Savannah type region - exhibits a more significant seasonal change in root zone soil moisture has been confirmed from the simulation results by [31] when assessing the SM and RR relationship in order to calibrate the Joint UK Land Environment Simulator (JULES) land surface model across the study area using satellite-based data from TAMSAT-ALERT (Tropical Applications of Meteorology using SATellite data and ground-based observations AgricuLtural dEcision suppoRT). For a detailed statistic of the SM and RR datasets, Fig. 3 shows a boxplot analysis of the SM/ RR pairwise datasets considering zonal and seasonal distribution scales. Figures 3a and 3b show the monthly total RR distribution across the climatic zones and seasons respectively. Firstly, the climatological average monthly total RR is unevenly distributed within and across zones and seasons, following the order 125.2

± 74.0 mm > 105.6 ± 69.0 mm > 103.4 ± 94.0 mm > 65.8 ± 55.0 mm for the Forest, Transition, Savannah, and Coastal climate zones respectively, with a seasonal variation in mean total RR in the order 153.6 ± 48.0 mm > 129.3 ± 48.0 mm > 112.3 ± 58.0 mm > 21.1 ± 8.0 mm for the JJA, MAM, SON, and DJF climatic seasons respectively. However invariably, contrary to the zonal RR distribution, Fig. 3c shows a monthly maximum zonal SM distribution following the order 0.79 ± 0.09 > 0.73 ± 0.07 > 0.66 ± 0.06 > 0.65 ± 0.06 for the Coastal, Forest, Transition, and Savannah climate zones respectively, while Fig. 3d shows the seasonal monthly maximum SM following the order 0.76 ± 0.06 > 0.69 ± 0.04 > 0.67 ± 0.06 > 0.6 ± 0.04 for the JJA, SON, MAM, and DJF climatic seasons respectively.

As seen, the SM - RR pairwise datasets show coherency in seasonal variation, and non-coherency in zonal variation, suggestive of a rather complicated SM - RR interplay. This apparent discrepancy can be resolved by considering that, a team of factors including prevailing climate [32], ecological conditions [33], topography [22, 23], and geography [34], as well as soil types and slopes, are contributing to the SM - RR interplay over the region. For example, [35] showed from observational experiments conducted over contrasting ecosystems in the loess hilly region of China that, highly forested areas with deep-rooted plants caused pronounced soil desiccation, while shrublands retained high soil water holding capacity, coupled with a strong regression slope between SM and RR. The study thus recommended shrubland types for land reclaim and vegetation restoration projects as they are more likely to protect the land from soil erosion. [36], also showed that soil water holding capacity decreased along inclined semi-arid regions of Inner Mongolia from the upper to lower areas after a rain event over the area, and depended inversely on the initial soil water.

However, the trend is shown in Figs. 3b and 3d suggests a strong positive linkage in the SM - RR relationship over the region, while Figs. 3a and 3c bring to bear the geographical and topographical effect in the SM - RR interplay. For example, the Coastal zone with the lowest RR over the region (Fig. 3a) would be expected to have low SM, while the Forest and Savannah zones have the highest SM, which is not entirely the case. Contrarily, the Forest zone is only second to the Coastal Zone with the Savannah zone showing the lowest zonal SM, accounting for the relative dryness towards the Sahel region shown in the Soil Moisture and Ocean Salinity (SMOS) and Aqua satellites [37].

3.2. Soil moisture and rainfall relationship considering rainfall onset

Figure 4 is a 30 years weekly averaged climatological time series for SM and RR over the four climatic zones, showing the mean rainfall onset dates as 19th, 12th, 13th, and 16th weeks across the Savannah, Transitional, Forest, and Coastal zones respectively. The onsets dates were determined based on the AGRHYMET's definition as the first rainy 10 days with at least a cumulative rainfall value of 25 mm, followed by less than 2–3 weeks dry spell [38]. It is worth mentioning that, these dates are long-term averages of station RR datasets over the zones and change by ± 23 days for each year. The objective here is to assess how onset dates feature in the SM - RR relationship, and thus attempt to establish a general

theoretical reference for application in agriculture as soil moisture is a key consideration factor in fixing planting dates [39].

Firstly, it is interesting to note from Fig. 4 that, SM follows closely the ITCZ - driven RR pattern for all the zones, namely, a bimodal over the southern half Coastal and Forest zones (Figs. 4c and 4d), intermediary over the Transitional zone (Fig. 4b), and mono-modal over the northern Savannah zone (Fig. 4a). However, the difference in SM and RR intensity changes during the onset week for each zone is remarkable. Table 2 summarizes the percentage changes in RR and SM during the onset week for each zone extracted from Fig. 4. The changes were determined with reference to the commencement of the year. The results show that, with the exception of the Coastal zone where an 86% rise in RR is commensurate with a 14% rise in SM, the Savannah and Forest zones show significantly low SM responses to RR, while the Transition zone shows a slight negative SM response of 0.01–99% increment in RR by the start of the season.

Table 2
Percentage change in RR and SM from the first week to onset week of the year for each climate zone

Zone	Mean onset	Percent change in RR during onset (%)	Percent change in SM during onset (%)
Savannah	19	98	0.04
Transition	12	99	-0.01
Forest	13	85	0.04
Coastal	16	86	14.00

The slightly negative and low responses for the stations in the Transitional, Savannah, and Forest zones respectively, may be attributed to SM deficits as a result of the high atmospheric evaporative power during the dry Harmattan season which commensurate with the boreal winter which climatologically extends from late November through to February [40–42].

The Harmattan season is characterized by low RR and intense atmospheric dryness along with strong dusty north-easterly winds developed from a continental scale pressure difference between the sub-tropical subsidence zone and the ITCZ, looming southward and lingering along the Gulf of Guinea [42].

Notably, during this period is the low atmospheric moisture convective activity and the consequential rainfall suppression which causes intense soil moisture stress due to high atmospheric evaporative power, strong dry winds, and low relative humidity [43]. Such environmental harsh conditions result in extremely low SM over the sub-region. The implication of this is that a large amount of RR is needed to satisfy the SM requirements to sufficiently support plant growth over the northern regions, and hence the amount of SM indicative of the start of rainfall season for planting time of various crops across the

zones cannot coincide. For example, [39] found a strong correlation between planting dates in April/ May and planting area with SM and RR over regions in northern Cambodia, and farmers thus resorted to earlier planting dates during wetter conditions.

3.3. Statistical assessment of the relationship between soil moisture and rainfall

Based on the observation data presented in Fig. 4, the relation between soil moisture (SM) and rainfall (RR) is expected to differ for each station. In order to quantify this relationship, Fig. 5 shows the results of station-by-station Pearson's correlation coefficients (r). Generally, from Fig. 5a, there is an all-positive correlation ranging between 0.38–0.82 ± 0.10, which peaks for the Savannah and Coastal stations at significant p-value < 0.05, while falling for the Transition and Forest stations. Following the example of [11] in the assessment of SM - RR relationship on a global scale using satellite data, the categorization of very strong positive (VSP = 0.8-1.0), strong positive (SP = 0.60–0.79), moderate positive (MP = 0.40–0.59), and weak positive (WP = 0.20–0.39) is used. One station shows a very strong positive SM – RR relationship, 14 stations show a strong positive SM-RR relationship, 6 stations show a moderate positive SM-RR relationship, while one more station is weak positive.

The variations in correlation coefficients are connected with the diverse and contrasting ecosystem conditions where stations are situated. In this regard, it is worth mentioning that, the results agree with the report by [11] using NASA's global SM and RR datasets, showing strong correlation coefficients over low vegetated regions and weaker correlation over highly forested regions. The weak correlations associated predominantly with the Forest climate stations can be attributed to the physical phenomenon of hydraulic redistribution where deep-rooted forested plants draw water from deep soil layers to surface root zone regions (100 cm) as a biological adaptation for dry season survival. [44] and [45] have described this condition for deeply rooted forested plants in the Congo Basin and Amazon respectively. Again, from Fig. 6, the very weak to moderate correlations are associated with the forested stations closer to the Volta River basin. Sehler [11] revealed that the geophysical process of river displacement - whereby rainfall over upper stream causes the lower stream end to expand, not necessarily due to RR, creates a condition of inverse SM - RR interplay, for areas nearby river systems. Conway [46] has illustrated this phenomenon in Eastern Africa, where heavy downpours over the Nile River are transported northward to Egypt and Sudan, causing elevated soil moisture not necessitated by rains in that area, thus yielding weak to negative SM - RR correlations.

Furthermore, from Fig. 6, the highest Pearson's correlation coefficient of 0.81 is associated with the Savannah climate, while all other stations show strong positive correlations > 0.61. The land cover type, geography, and topographic features are expected to allow for such high positive correlations as reported by [11] for other regions with similar climates and land cover. In practice, [41] realized this from soil moisture measurements at eddy covariance stations in Sudanian Savannah ecosystems across the West Africa terrain. They reported high variability and quick response of SM to RR, mainly due to the variability in vapour pressure deficit over the region. Overall, whereas one Savannah stations show a very strong

positive SM - RR relationship, and one Forest station shows a week positive, the larger number of stations across the study area shows moderate to strong positive correlation.

Conclusion

The study presents an assessment of soil moisture (SM) and rainfall (RR) interplay over different tropical climate zones across Ghana in the West African terrain. This was achieved using gauge measurements for 22 Synoptic stations from the Ghana Meteorological Agency spanning 30 years (1990 - 2019), and satellite-based datasets of root zone soil moisture at 100 cm depth retrieved from the National Aeronautics and Space Administration - Prediction of Worldwide Energy Resources (NASA/ POWER) agro-climatological archives spanning equal period as the gauge dataset, accessible on a daily and monthly temporal resolution scale at $0.5^{o} \times 0.5^{o}$ spatial resolution. The SM - RR spatiotemporal distributions, percentage changes in relation to onset dates, and statistical strength of correlations were presented and discussed. It is shown that, generally, SM and RR show moderate to strong positive correlations in the range of 0.38 - 0.82 ± 0.10 across the study area, with the highest correlations over the northern Savannah and Coastal Savannah, while the weakest correlations are mainly for stations in the Forest zones, in tandem with the global SM - RR relationships report by [11]. The weak to low correlations have been associated with soil-plant ecological adaptation as pointed out in other studies [45-44]. Moreover, it is shown that when the rainfall season onset dates were averaged over the zones, the Coastal zone exhibits the highest percentage change in SM at 14%, whereas the Forest, Transition, and Savannah zones exhibit low to slightly negative percentage changes in SM at 0.04%, -0.01%, and 0.04% respectively. This has been attributed to SM deficits caused by the lingering dryness effect of the Harmattan season preceding the onset date. Doubtless, the study unravels complexities in the SM - RR interplay over the region, occasioning the assertion that the soil moisture and rainfall relationship is rather more complicated. Additionally, based on the low correlation results for highly forested regions vis-à-vis reports from literature, and also considering the fact that this study used only 22-point stations which are limited in terms of the spatial coverage, negative correlations are possible, and from the time series analysis, suggested possible reason has been stated as SM increase not accentuate by RR. The spatiotemporal display and time series evaluation offered useful insights in showing that SM - RR interplay is significantly variable for each climate zone. For instance, the Savannah stations will require more SM to satisfy a suitable onset date for planting, whereas the Coastal zone will not require much SM to satisfy such requirements. Further, low SM - RR correlations over the Forest zone have been attributed to geophysical phenomena of hydraulic redistribution as identified by [45] and [44] and river displacement [46]. Overall, the study unravels key characteristic features in SM-RR interplay over the tropical sub-region which have immense theoretical and practical importance for ecosystem water resource assessment and sustainability, soil water environmental protection, drought and drought-related stress monitoring and prediction, and pluvial flood prevention over the sub-region.

Declarations

Data availability

The datasets used and/or analyzed during the current study are available from the corresponding author on reasonable request.

Acknowledgments

We are thankful for the long-term NASA/ POWER root zone soil moisture satellite-based reanalysis datasets obtained from the NASA Langley Research Center POWER Project funded through the NASA Earth Science Directorate Applied Science Program. The datasets are assessable at https://power.larc.nasa.gov/data-access-viewer/.

We are also thankful for the ground station gauge rainfall measurement datasets received from the Ghana Meteorological Agency (GMet).

Author contributions

P. J. A. and F. D conceptualized the work, retrieved and quality controlled satellite and gauge measurement datasets, and wrote manuscript. E. Q supervised the findings of this work. D. A. organized manuscript content per Journal requirements. All authors discussed the results and contributed to the final manuscript.

Competing interests

The authors declare no competing interests.

References

1. Pan, N., Wang, S., Liu, Y., Zhao, W., & Fu, B. Global surface soil moisture dynamics in 1979–2016 observed from ESA CCI SM dataset. *Water***11**, 883 (2019).
2. Myeni, L., Moeletsi, M. E., & Clulow, A. D. Development and analysis of a long-term soil moisture data set in three different agroclimatic zones of South Africa. *Afr. J. Sci.***117**, 1-8 (2021).
3. Orth, R., & Seneviratne, S. I. Using soil moisture forecasts for sub-seasonal summer temperature predictions in Europe. *Dyn.* **43**, 3403-3418 (2014).
4. Silvestro, F., et al. Impact-based flash-flood forecasting system: Sensitivity to high resolution numerical weather prediction systems and soil moisture. *Hydrol.***572**, 388-402 (2019) .
5. Lu, N., Chen, S., Wilske, B., Sun, G., and Chen, JEvapotranspiration and soil water relationships in a range of disturbed and undisturbed ecosystems in the semi-arid Inner Mongolia, China. *Plant Ecol*. **4**, 49-60 (2011).
6. Nikam, B. R., Kumar, P., Garg, V., Thakur, P. K., and Aggarwal, S. P. Comparative evaluation of different potential evapotranspiration estimation approaches. *J. Res. Eng. Technol***3**, 544-552 (2014).

7. Kabo-bah, A. T., Anornu, G. K., Ofosu, E., Andoh, R., and Lis, K. J. Spatial-temporal estimation of evapotranspiration over Black Volta of West Africa. *J. Water Res. Environ. Eng*. **6**, 295-302 (2014).
8. Petropoulos, G. P., Srivastava, P. K., Piles, M., & Pearson, S. Earth observation-based operational estimation of soil moisture and evapotranspiration for agricultural crops in support of sustainable water management. *Sustainability***10**, 181 (2018).
9. Wasko, C., & Nathan, R. Influence of changes in rainfall and soil moisture on trends in flooding. *Hydrol*. **575**, 432-441 (2019).
10. Gohain, K. J., Mohammad, P., & Goswami, A. Assessing the impact of land use land cover changes on land surface temperature over Pune city, India. *Int*. **575**, 259-269 (2021)
11. Sehler, R., Li, J., Reager, J. T., & Ye, H.. Investigating relationship between soil moisture and precipitation globally using remote sensing observations. *Contemp. Water Res. Educ.***168**, 106-118 (2019).
12. Yang, L., Sun, G., Zhi, L., & Zhao, J. Negative soil moisture-precipitation feedback in dry and wet regions. *Rep*. **8**, 1-9 (2018).
13. Cook, B. I., Bonan, G. B., & Levis, S. Soil moisture feedbacks to precipitation in southern Africa*. J. Clim*. **19**, 4198-4206 (2006)
14. Masih, I., Maskey, S., Mussá, F. E. F., & Trambauer, P. A review of droughts on the African continent: a geospatial and long-term perspective. *Earth Syst. Sci.***18**, 3635-3649 (2014).
15. Klutse, N. A. B., Owusu, K., & Boafo, Y. A. Projected temperature increases over northern Ghana. *SN Appl. Sci*. **2**, 1-14 (2020).
16. Liu, Y. & Xue, Y. Expansion of the Sahara Desert and shrinking of frozen land of the Arctic. *Rep*. **10**,1-9 (2020).
17. Amekudzi, L. K. et al. Variabilities in rainfall onset, cessation and length of rainy season for the various agro-ecological zones of Ghana*. Cli*. **3**, 416-434 (2015).
18. Asilevi, P. J., Quansah, E., Amekudzi, L. K., Annor, T., & Klutse, N. A. B. Modeling the spatial distribution of Global Solar Radiation (GSR) over Ghana using the Ångström-Prescott sunshine duration model. *Afri*. **4**, e00094 (2019).
19. Asante, F. A. & Amuakwa-Mensah, F. Climate change and variability in Ghana: Stocktaking. *Clim*. **3**, 78-99 (2015).
20. Klein, C., Heinzeller, D., Bliefernicht, J. & Kunstmann, H. Variability of West African monsoon patterns generated by a WRF multi-physics ensemble. *Dyn.***45**, 2733-2755 (2015).
21. Hill, P. G., Allan, R. P., Chiu, J. C. & Stein, T. H. A multi-satellite climatology of clouds, radiation, and precipitation in southern West Africa and comparison to climate models*. J. Geophys. Res.*: *Atmos*. **121**, 10-857 (2016).
22. Jin, Z., Guo, L., Lin, H., Wang, Y., Yu, Y., Chu, G., & Zhang, J. Soil moisture response to rainfall on the Chinese Loess Plateau after a long-term vegetation rehabilitation. *Process*. **32**, 1738-1754 (2018).

23. Guo, X. et al. Spatial variability of soil moisture in relation to land use types and topographic features on hillslopes in the black soil (mollisols) area of northeast China. *Sustainability*, **12**, 3552 (2020).
24. Rhebergen, T. et al. Climate, soil and land-use based land suitability evaluation for oil palm production in Ghana. *Eur J. Agron*. **81**, 1-14 (2016).
25. Reichle, R. H. et al. Assessment of MERRA-2 land surface hydrology estimates. *Clim*. **30**, 2937-2960 (2017).
26. Gelaro, R. et al. The modern-era retrospective analysis for research and applications, version 2 (MERRA-2). *Clim*. **30**, 5419-5454 (2017).
27. Obilor, E. I. & Amadi, E. C. Test for significance of Pearson's correlation coefficient. *J. Innov. Math. Stat. Energy Policies,* **6**, 11-23 (2018).
28. Andrade, C. Understanding the difference between standard deviation and standard error of the mean and knowing when to use which. *Indian J. Psychol. Med.* **42,** 409-410 (2020).
29. Addi, M. et al. Impact of large-scale climate indices on the meteorological drought of coastal Ghana. *Meteorol*. (2021).
30. Sakyi, P. A., Asare, R., Fynn, O. F. & Osiakwan, G. M. Assessment of groundwater quality and its suitability for domestic and agricultural purposes in parts of the Central Region, Ghana. *West Afr. J. Appl. Ecol*. **24**, 67-89 (2016).
31. Pinnington, E., Quaife, T. & Black, E. Impact of remotely sensed soil moisture and precipitation on soil moisture prediction in a data assimilation system with the JULES land surface model. *Earth Syst. Sci*. **22**, 2575-2588 (2018).
32. Humphrey, V. et al. Soil moisture–atmosphere feedback dominates land carbon uptake variability. *Nature,***592**, 65-69 (2021).
33. Su, B., & Shangguan, Z. Decline in soil moisture due to vegetation restoration on the Loess Plateau of China. *Land Degrad. Dev*. **30**, 290-299 (2019).
34. Liu, T. W. et al. Conversion relationship of rainfall-soil moisture-groundwater in Quaternary thick cohesive soil in Jianghan Plain, Hubei Province, China. *China Geol*. **3**, 462-472 (2020).
35. Cheng, R. R. et al. Soil moisture variations in response to precipitation in different vegetation types: A multi-year study in the loess hilly region in China. **13**, e2196 (2020).
36. Zhang, Y. et al. The response of soil moisture content to rainfall events in semi-arid area of Inner Mongolia. *Procedia Environ. Sci*.**2**, 1970-1978 (2010)
37. Klemas, V., Finkl, C. W., & Kabbara, N. Remote sensing of soil moisture: An overview in relation to coastal soils. *Coast. Res***30**, .685-696 (2014).
38. Ojo, O. I., & Ilunga, M. F. Application of nonparametric trend technique for estimation of onset and cessation of rainfall. *Air Soil Water Res*. **11**, 1–4, 1178622118790264 (2018).
39. Tsujimoto, K. et al. Multiyear analysis of the dependency of the planting date on rainfall and soil moisture in paddy fields in Cambodia, 2003–2019. *Paddy Water Environ*. **19**, 635-648 (2021).

40. He, C., Breuning-Madsen, H., & Awadzi, T. W. Mineralogy of dust deposited during the Harmattan season in Ghana. *Tidsskr*. **107**, 9-15 (2007).
41. Quansah, E. et al. Carbon dioxide fluxes from contrasting ecosystems in the Sudanian Savanna in West Africa. *Carbon Balance Manag*. **10**, 1-17 (2015).
42. Della Sala, P. et al. Assessment of atmospheric and soil water stress impact on a tropical crop: the case of Theobroma cacao under Harmattan conditions in eastern Ghana. *For. Meteorol*. **311**, 108670 (2021).
43. Schepanski, K., Heinold, B. & Tegen, I. Harmattan, Saharan heat low, and West African monsoon circulation: modulations on the Saharan dust outflow towards the North Atlantic. *Chem. Phys*. **17**, 10223-10243 (2017).
44. Yan, B. & Dickinson, R. E. (2014). Modeling hydraulic redistribution and ecosystem response to droughts over the Amazon basin using Community Land Model 4.0 (CLM4). *Geophys Res.: Biogeosciences*, 119(11), 2130-2143.
45. Harper, A. B. et al. Role of deep soil moisture in modulating climate in the Amazon rainforest. *Geophys Res*. Lett. **37**, (2010). Conway, D. The climate and hydrology of the Upper Blue Nile River. *Geogr. J*. **166**, 49-62 (2000).

Figures

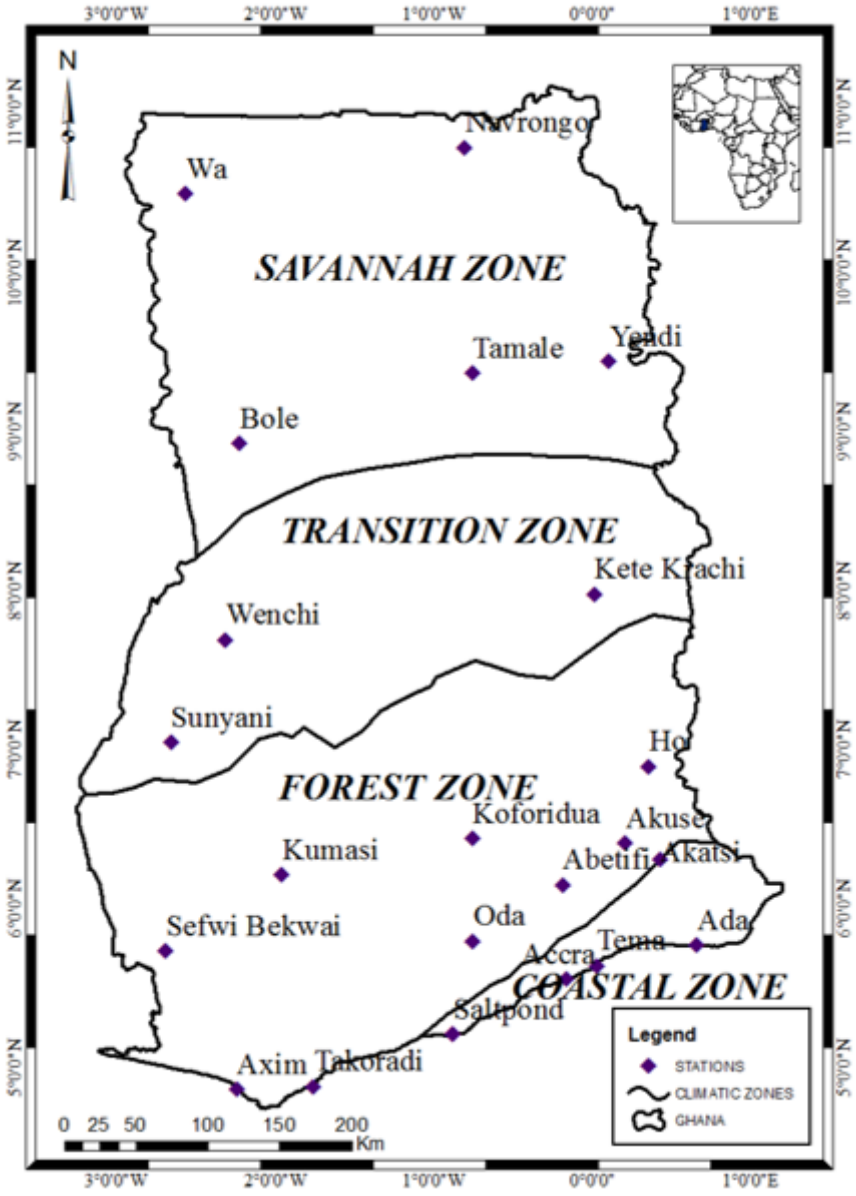

Figure 1

Map of the study area showing all twenty-two (22) synoptic stations distributed in four main climatological zones countrywide. Adapted from [18]

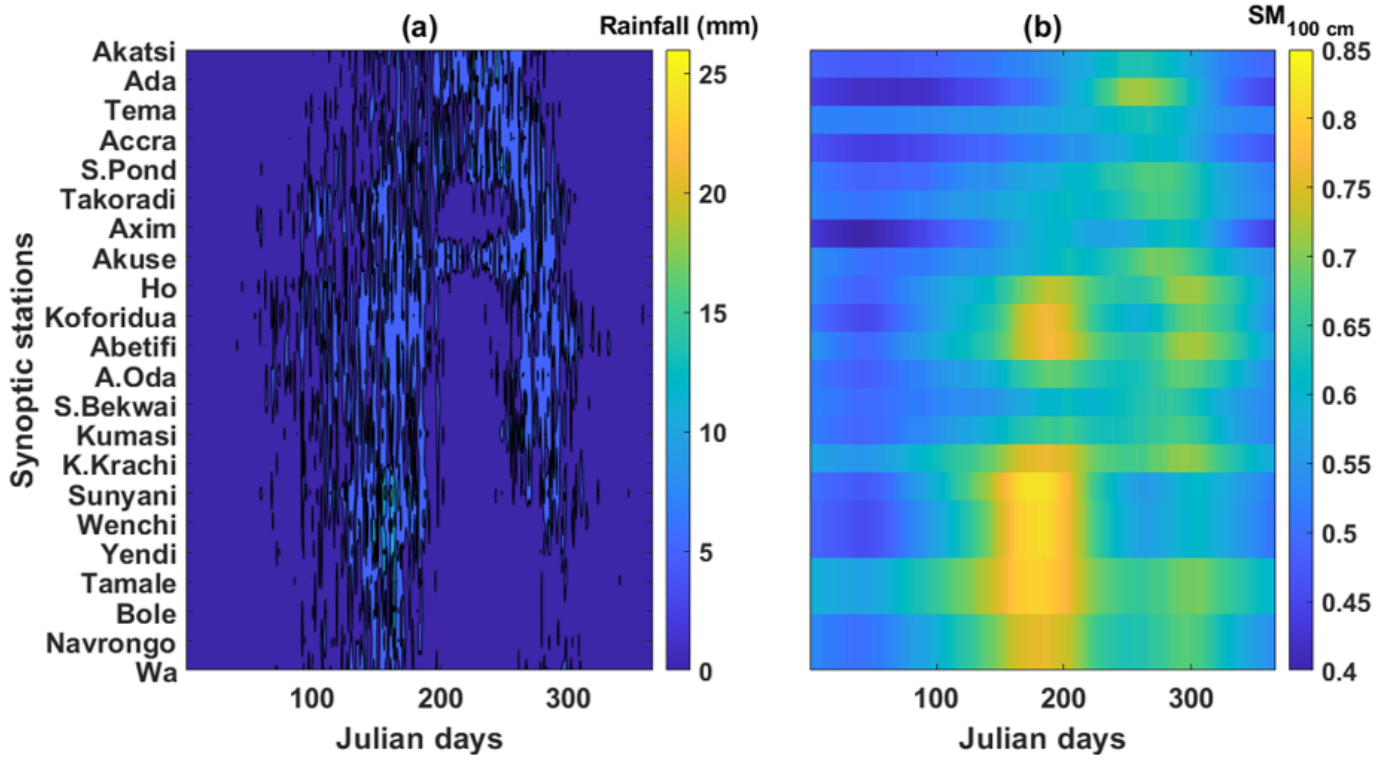

Figure 2

Climatological spatiotemporal distribution of daily (a) root zone soil moisture at 100 cm depth (SM_{100}) and (b) rainfall (RR) at all 22 synoptic stations. Here, SM_{100} = 0 represents a water-free soil and a SM_{100} = 1 represents saturated soil. Station codes follow the order - Savannah to Coastal - presented in Table 1

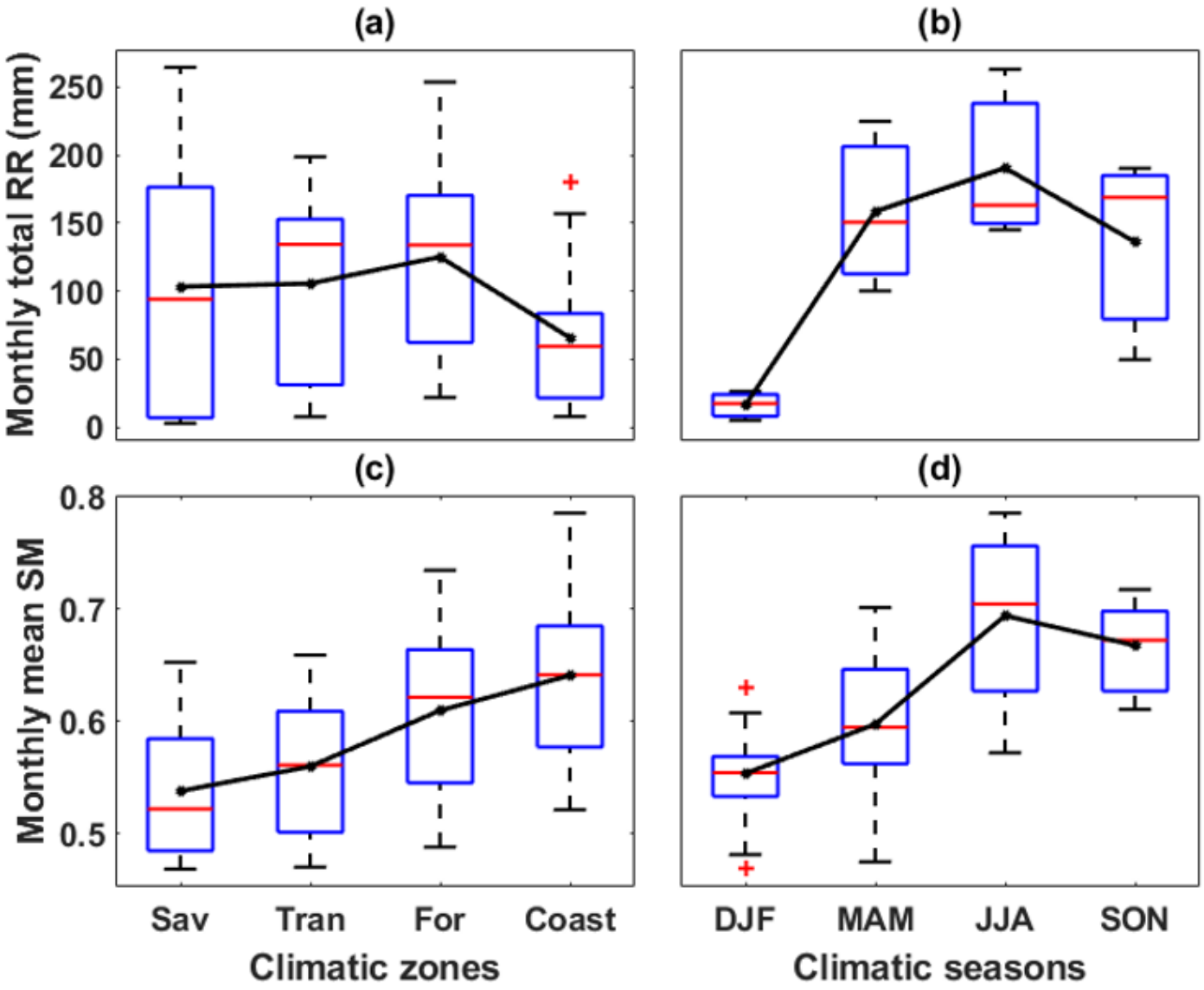

Figure 3

Boxplots comparing climatological (a) zonal monthly total RR, (b) seasonal monthly total RR, (c) zonal monthly mean SM, and (d) seasonal monthly mean SM distribution over the study area. Trend line shows the mean.

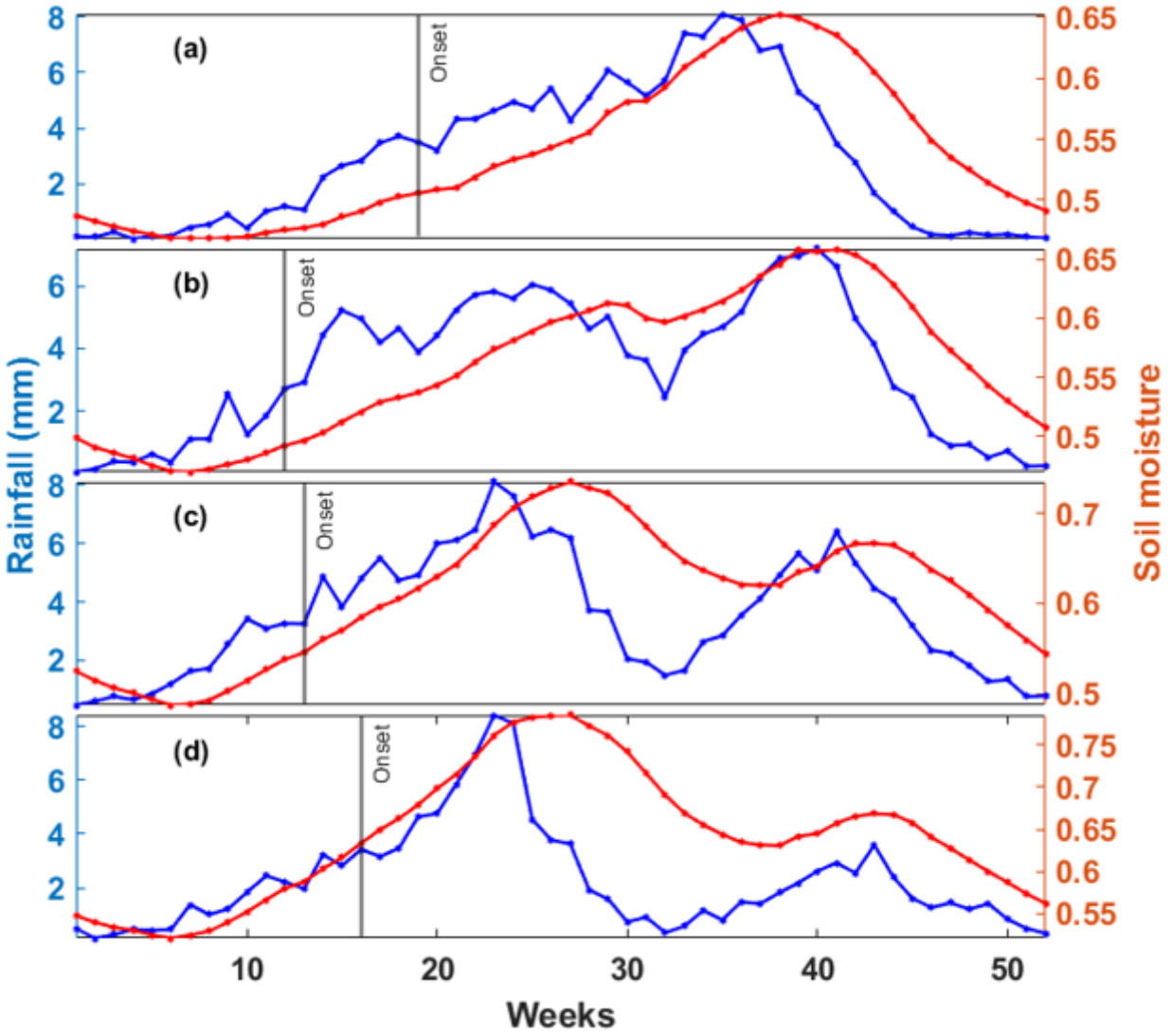

Figure 4

Time series plot comparing climatological weekly averages of SM and RR over the (a) Savannah, (b) Transition, (c) Forest, and (d) Coastal climatic zones

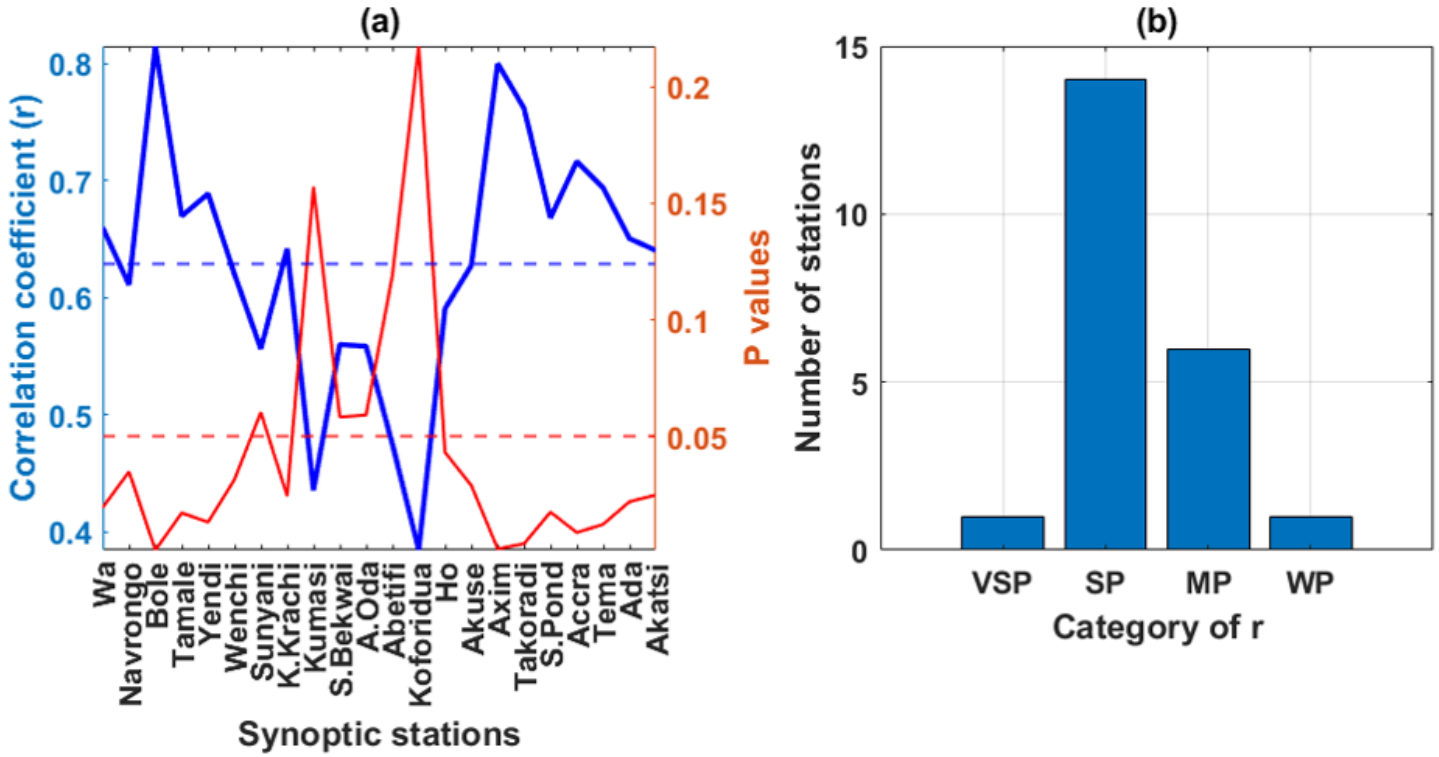

Figure 5

(a) Station-by-station SM - RR Pearson's correlation coefficients (r) with significant p-values (< 0.05) showing mean r and p as broken lines and (b) the total number of stations showing very strong positive (0.8-1.0), strong positive (0.60-0.79), moderately positive (0.4-0.59), and weak positive (0.20-0.39) r for SM - RR

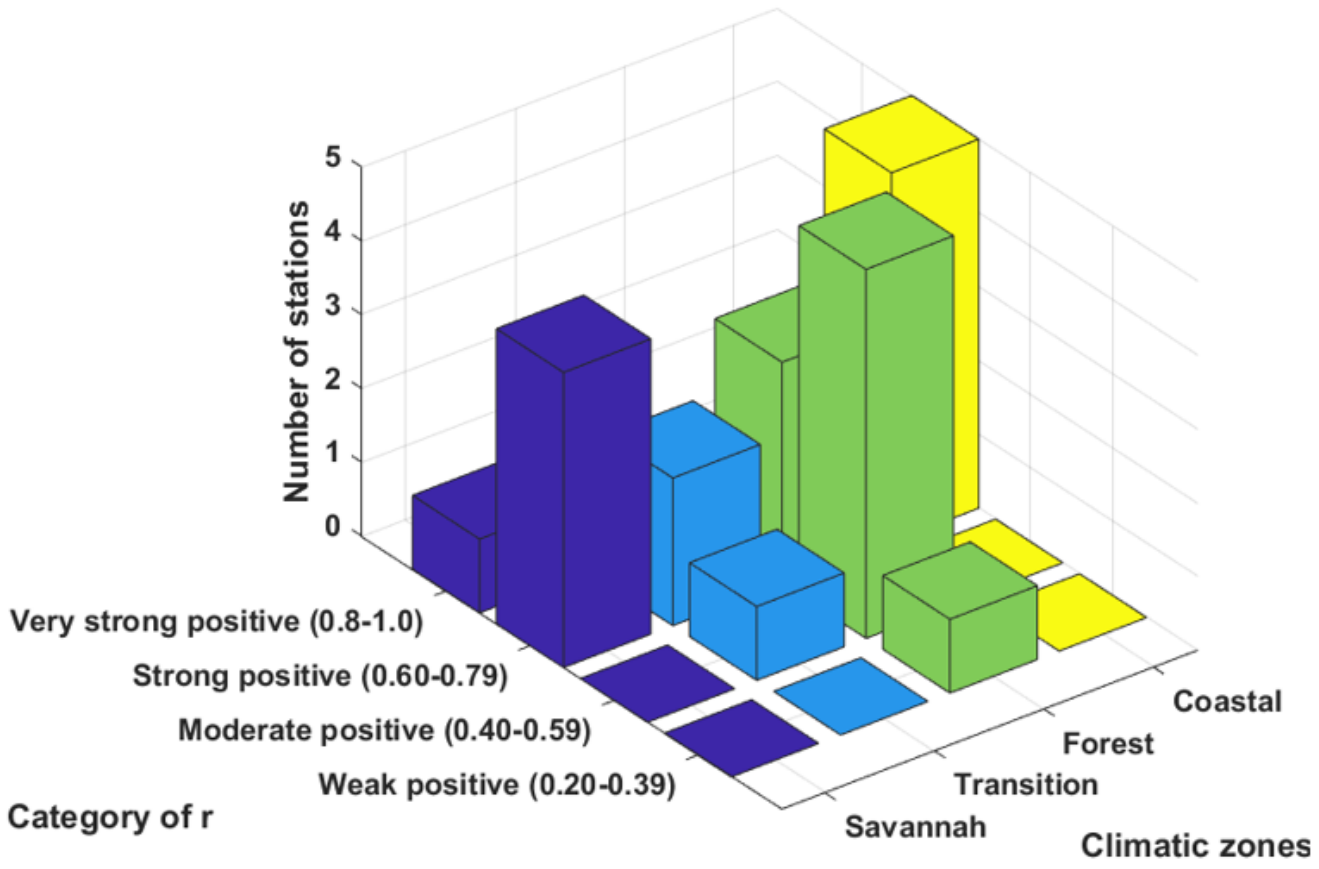

Figure 6

Zonal classification of SM - RR Pearson's correlation coefficients (r) for very strong positive (0.8-1.0), strong positive (0.60-0.79), moderate positive (0.40-0.59), and weak positive (0.20-0.39)